# Cycloadditions on Diamond (100) 2 × 1: Observation of Lowered Electron Affinity due to Hydrocarbon Adsorption

**Ti Ouyang,[†] Xingyu Gao,[‡] Dongchen Qi,[‡] Andrew Thye Shen Wee,[‡] and Kian Ping Loh*[,†]**

*Department of Chemistry and Department of Physics and the Singapore Synchrotron Light Source, National University of Singapore, 3 Science Drive 3, Singapore 117543*

*Received: November 23, 2005; In Final Form: January 23, 2006*

The adsorption of allyl alcohol, acrylic acid, and allyl chloride, as well as unsaturated organic molecules such as acetylene and 1,3 butadiene, on reconstructed diamond (100) 2 × 1 have been investigated using high-resolution electron energy loss (HREELS) spectroscopy and synchrotron radiation spectroscopy. The cycloadditions of these organic molecules produce chemically adsorbed adlayers with varying degree of coverages on the clean diamond. The organic adsorbed surface has a lowered electron affinity and shows a secondary electron yield that varies between 12 and 40% of the yield obtained from a fully hydrogenated diamond surface. The diamond surface can be functionalized with hydroxyl, carboxylic, and chlorine functionalities by the adsorption of these allyl organics. The [2 + 2] adduct of acetylene on the diamond (100) 2 × 1 surface can be observed. 1,3-Butadiene attains a higher coverage as well as forms a thermally more stable adlayer on the diamond surface compared to the other organic molecules, due to its ability to undergo [4 + 2] cycloaddition.

## 1. Introduction

The biocompatibility and wide electrochemical potential window of diamond has generated a lot of interest in the surface functionalization of diamond, with a view to its potential applications in bioelectronics,[1,2] electrochemistry[3], and pH sensors.[4] In addition to bulk properties such as hardness, optical transparency, and wide band gap, diamond enjoys unique surface properties such as negative electron affinity and *p*-type surface conductivity.[5−7] There are several routes whereby surface functionalization can be achieved. Jian and co-workers[8] performed the electrochemical reduction of aryldiazonium salts on nanocrystalline diamond and demonstrated the covalent coupling of the functionalized surface to DNA and proteins. Strother and co-workers[9] used ultraviolet light to initiate a coupling reaction between a hydrogen-terminated diamond surface and functionalized alkenes. This reaction mechanism is motivated by the principle that photoattachment reactions can be initiated via photoexcitation of electrons and holes in the surface space-charge region, followed by nucleophilic attack by an alkene at the surface.[10]

Cycloaddition reactions constitute a powerful method for the formation of C−C bonds and could provide a means for the controlled functionalization of $\pi$-reconstructed diamond surfaces. It has been proposed that the reconstructed, clean C(100) 2 × 1 surface is ideal for studying the Diels−Alder reaction because the dimer is unbuckled. Diels−Alder reactions on clean diamond (100) 2 × 1 has been investigated previously by Hossain and co-workers,[11] their EELS studies showed that 1,3-butadiene readily chemisorbed on the C(100) 2 × 1 surface by [4 + 2] type cycloaddition, but the [2 + 2] cycloadditions of ethylene, ethyne, and benzene to the (100) 2 × 1 surface were not favored because it is symmetry-forbidden. As a result they concluded that the orbital symmetry of the reacting species determines the reaction probability. This conclusion was supported by the FTIR study of Wang and co-workers.[12] Hovis and co-workers[13] studied the reaction of cyclopentene with diamond and demonstrated using FTIR spectroscopy that a [2 + 2] cycloaddition product can be generated. However, they reported that the sticking coefficient of cyclopentene on diamond is in the order of $10^{-3}$, which is several orders of magnitudes lower than that of Ge and Si. The lower reaction probability on diamond compared to Si and Ge is probably associated with its larger band gap and the absence of dimer tilting on its surface; dimer tilting facilitates the ability of the impinging nucleophilic reactants to find a low-symmetry pathway to the final [2 + 2] reaction product.[14−18] The very low sticking coefficient, however, was commented on by Carbone[19] to be caused by the adsorption of cyclopentene on defects rather than dimers. Calculations by Cho and Kleinman[17,18] showed that the reaction barrier for the cycloaddition of $C_2H_4$ on C(100) is as high as 0.9 eV and the sticking coefficient to be lower than $10^{-15}$ at room temperature.

The diamond surface can be considered as a solid organic template, and the ordered adsorption of hydrocarbon molecules for example can be considered as an extension of the diamond surface lattice due to the C−C covalent coupling at the interface. In the past, attention was focused mainly on the effects produced by chemisorbed hydrogen and oxygen on the electron affinity, surface conductivity, and reactivity of diamond. The presence of hydrogen for example has been found to induce hole accumulation on the surface and generate a *p*-type conducting channel on the surface.[20,21] The chemisorption of hydrogen also introduces the condition of negative electron affinity (NEA).[22−27] The effects produced by adsorbed hydrocarbons on the surface electronic properties of diamond have not been documented.

The Diels−Alder reaction[8−11] has generality toward a large variety of substituents on both the diene and the dienophile

* To whom correspondence should be addressed. E-mail: chmlohkp@nus.edu.sg.
[†] Department of Chemistry.
[‡] Department of Physics and the Singapore Synchrotron Light Source.

10.1021/jp056785i CCC: $33.50 
Published on Web 02/28/2006

(allene). The reaction works best when the two reactants are electronically complementary; i.e., one of them is electron rich, while the other is electron poor. Allenes of the class A−$CH_2$−X, where A = $CH_2$═CH and X = OH, COOH, and Cl, are bifunctional compounds. The A moiety consists of unsaturated $\pi$ bonds which can undergo the usual Diels−Alder reaction, while the X moiety can constitute a wide range of functional groups that activate or deactivate electrophilic addition via inductive effects. If the cycloaddition of these compounds to the dimer bonds of C(100) 2 × 1 is possible, then the addition of allenes provide a powerful way to functionalize the diamond surfaces in a controlled manner due to the ease of varying the functional group X.

In this work, we study the chemisorption of a range of organic compounds which can potentially undergo cycloadditions with diamond; these include allyl organics such as allyl alcohol, acrylic acid, and allyl chloride, as well as 1,3-butadiene and acetylene. The surface adsorption of these organics has been verified by high-resolution electron energy loss spectroscopy (HREELS) as well as synchrotron radiation spectroscopy.

## 2. Experimental Section

The diamond sample used in this study was a 4 mm × 4 mm boron-doped single-crystal diamond (100) grown epitaxially on type IIb diamond single-crystal substrate. The diamond was first cleaned with microwave hydrogen plasma at 800 °C before introduction into a ultrahigh-vacuum preparation chamber equipped with low-energy electron diffraction (LEED) optics and gas dosing facilities. The diamond crystal was flash-annealed to 1000 °C to prepare a C(100) 2 × 1 surface, as verified by LEED. A dosing tube was used to dose organic molecules onto the surface via a precision leak valve. The dosing was usually carried out at room temperature unless specified otherwise. After dosing, the diamond sample was immediately transferred via a gate valve into an adjoining ultrahigh-vacuum chamber for high-resolution electron energy loss spectroscopy (SPECS GmbH Delta 0.5). The primary electron energy was set at 5 eV. The full width at half-maximum was 8 meV for the bare diamond. Photoelectron spectroscopy and X-ray adsorption spectroscopy (XAS) were carried out at the SINS beam line of the Singapore Synchrotron Light Source.[28] The base pressure in both the HREELS chamber and the synchrotron radiation spectroscopy chamber was $1 \times 10^{-11}$ Torr.

The HREELS spectra for the same series of measurements were normalized to their respective elastic peak intensity. The binding energies in photoelectron spectroscopy were referred to the Au $4f_{7/2}$ peak or the Fermi edge of a gold foil attached to the sample. A Shirley background subtraction was performed for the XPS spectra. The spectra were subsequently peak-fitted using mixed Lorentzian and Gaussian line shapes.

## 3. Result

**3.1. Covalent Functionalization of the Diamond (100) 2 × 1 surface by Allyl Organics.** Figure 1 show the loss intensities for the C(100) 2 × 1−H as a function of primary beam energy. The hydrogen-plasma polished C(100) 2 × 1−H surface typically consists of several peaks in the HREELS spectrum, as shown in Figure 1a. These include the C−H stretching at 363.4 meV, C−H bending at 176.5 meV, and a C−H twisting mode of the H-terminated dimer at 145.8 meV ($B_1$) which overlaps with the bulk TO phonon at 136 meV.[29] The signal at 112.0 meV ($S_1$) is assigned to a surface phonon mode related to dimer scissoring on C(100) 2 × 1−H; this mode disappears after annealing to hydrogen desorption temperatures.

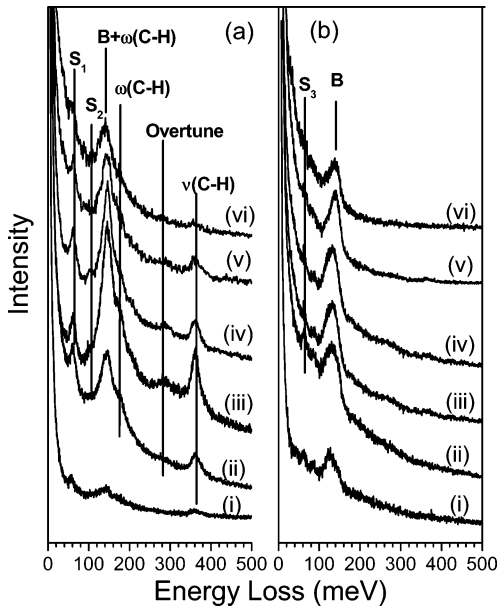


**Figure 1.** Plot of HREELS loss intensities versus primary beam energy ($E_p$) for (a) hydrogenated diamond C(100) 2 × 1−H and (b) bare diamond C(100) 2 × 1 at $E_p$ of (i) 3, (ii) 5, (iii) 8, (iv) 10, (v) 15, and (vi) 20 eV. B: bulk phonon TO at X. S1, S2, and S3: surface dimers.

The broad, weak signal at 280 meV is assigned to an overtone of C−H bending modes around 140 meV; such a structure was not observed in the HREELS spectrum of bare diamond. The loss intensities for the C(100) 2 × 1−H shows significant dependence on primary electron energy, indicating that resonance scattering occurs. The hydrogenated diamond shows negative electron affinity (NEA); thus it is possible that incoming electrons can populate the conduction bands and be scattered efficiently at some resonance energies. Our observation agrees with the energy dependence of the loss intensities observed by Thachepan and co-workers in their HREELS study of hydrogenated diamond.[29]

After the diamond was annealed to hydrogen-desorption temperature (i.e. 1000 °C), all the C−H modes shown in Figure 1a disappear. Figure 1b shows that the energy loss peaks of the bare surface consist of two surface phonons at 62.5 meV ($S_2$, dimer out-of-phase bouncing) and 86.5 meV ($S_3$, dimer in-phase bouncing) and a diamond bulk phonon ($B_2$, TO at X) at 134.1 meV.[30,31] For the clean diamond surface which is well-known to exhibit the condition of positive electron affinity, it is apparent from Figure 1b that the loss intensities show no obvious dependence on the primary beam energy.

After the dosing of various organic molecules on the surface, the bare diamond surface phonons at 62.5 and 86.5 meV decrease in intensity. The newly appeared vibration modes following the saturation dose of organic molecules such as acrylic acid, allyl alcohol, 1,3 butadiene, acetylene, and allyl chloride are summarized in Table 1. Parts a−f of Figure 2 show the composite spectra where we superimpose the plots from different dosing experiments for ease of comparison. After exposure to acrylic acid (Figure 2c), new peaks are observed at 209.6 meV (C═O stretching), 366.0 + 381.7 meV (C−H stretching), 176.2 meV (C−H bending), and 120.7 meV (C−O stretching, overlapping with peaks around 140 meV, due to a mixture of diamond phonon and C−H bending signals). After adsorption of allyl alcohol, new vibration peaks that appear include C−O stretching, C−H stretching, C−H bending, and C═C stretching, as shown in Figure 2d. The absence of a distinct −OH stretching peak around 430 meV is probably due to the

**TABLE 1: HREELS Peak Positions after Saturation Dosage of Various Organic Molecules on the Diamond C(100) 2 × 1 Surface[a]**

| | HREELS peak position for given organic molecules (meV) | | | |
|---|---|---|---|---|
| | 1,3-butadiene | acrylic acid | allyl alcohol | acetylene |
| C−H streching | 365.1 + 382.7 | 366.0 + 381.7 | 365.5 + 379.9 | 382.1 |
| C−H bending | 178 | 176.2 | 174.4 | 179.8 |
| C═C streching | 202.1 | | 202.1 | 203.1 |
| C═O streching | | 209.6 | | |
| C−O streching | | 120.7 | 120.3 | |

[a] No results were obtained for allyl chloride.

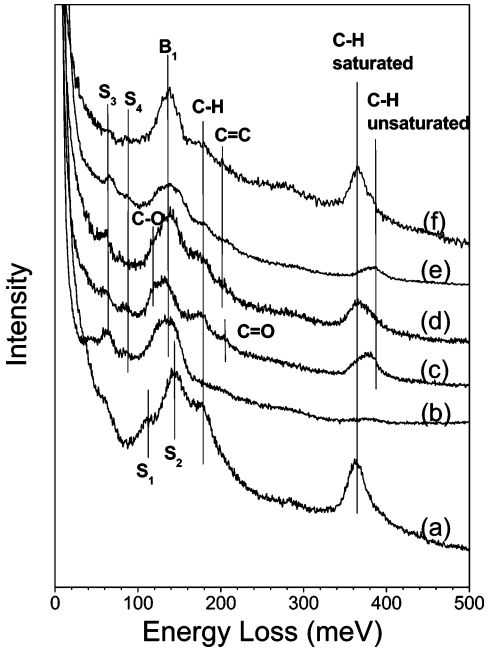


**Figure 2.** HREELS spectra of (a) C(100) 2 × 1−H; (b) C(100) 2 × 1; and after saturation exposure to (c) acrylic acid, (d) allyl alcohol, (e) acetylene, and (f) 1,3-butadiene. $S_1$: surface dimer phonon, scissoring. $S_2$: surface dimer phonon, twisting. $S_3$: dimmer, out-of-phase bouncing. $S_4$: dimmer, in-phase bouncing. $B_1$: longitudinal bulk phonon at X.

formation of hydrogen bonding among O−H bonds; this will broaden the peak and shift the vibration toward lower frequency, and thus the O−H vibration signal could be merged with the C−H stretching peak.[32] The presence of a weak feature assignable to the C═C stretching mode in the spectrum of some of the organic molecules are probably due to multilayer adsorption. It is noteworthy that for acrylic acid and acetylene, the C−H stretching is observed to shift toward higher wavenumber at 380 meV, compared to that of hydrogenated diamond at 363 meV. For acetylene, which is shown in Figure 2e, the energy loss of the C−H stretching peak (382.1 meV) lies in the range of $sp^2$ carbon atoms and the existence of C═C vibration suggests the unsaturated nature of the bonds. The HREELS spectrum of 1,3-butadiene in Figure 2f agrees well with literature,[11] the C−H bending and C−H stretching peaks exhibit stronger intensity compared to that of the other organic molecules.

Synchrotron radiation spectroscopy was used to study the evolution of new species on the diamond surface after dosing the above-mentioned molecules. The shape changes in the C1s core level, as well as associated chemical shifts of the C1s peak after dosing with the organic molecules, are shown in Figure 3. For the hydrogen-terminated C(100) 2 × 1-H surface, Figure 3a shows the presence of only one bulk peak at 284.4 eV. After

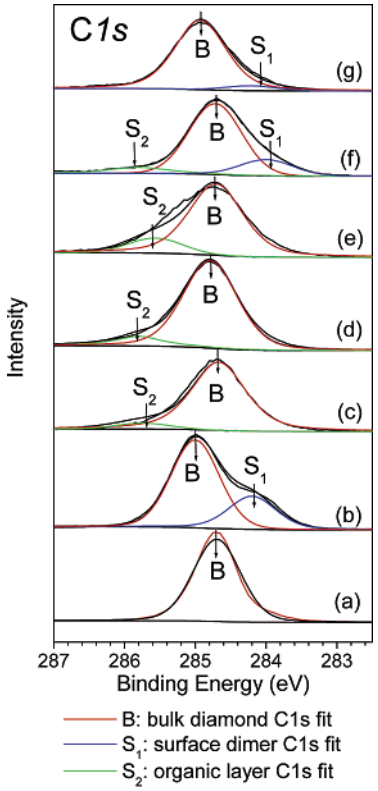


**Figure 3.** C1s core level spectra of (a) hydrogenated diamond C(100) 2 × 1; (b) bare diamond C(100) 2 × 1; and after saturation dosing of a variety of organics: (c) allyl chloride, (d) acrylic acid, (e) allyl alcohol, (f) acetylene, and (g) 1,3-butadiene. B: C1s of bulk diamond. $S_1$: C1*i* of surface dimer. $S_2$: C1s of the organic layer formed by dosing various organic molecules.

annealing to 1000 °C, the bulk C1s peak shifts to 285.0 eV; there is also a chemically shifted peak at 284.2 eV assignable to the reconstructed surface dimer. The peak position due to the C1s dimer is 0.7−0.8 eV lower than that of the bulk C1s, while the peak area is 30−40% of the bulk at the surface-sensitive photon energy of $h\nu = 350$ eV at normal incidence (with source to analyzer angle of 54°). The origin of this chemical shift arises from the more effective shielding of the photogenerated hole by the $\pi$ electrons in the surface dimer bonds; the extra energy gain in terms of this interatomic relaxation results in an increase in kinetic energy of the photoelectrons originating from the surface dimers, i.e., a shift to lower binding energy. It has been reported that the bare diamond surface shows downward band bending due to hole depletion, while hydrogen termination reduces the downward band bending due to hole accumulation. In this case, the increase of the bulk C1s binding energy after annealing to hydrogen-desorption temperature agrees with the increased downward band bending.[24]

Following the saturation dosage of organic molecules on the bare diamond surface, the dimer peak disappeared, as shown in Figure 3c−g. At the same time, a new peak appeared at the higher binding energy side of the C1s peak for all molecules other than 1,3-butadiene. These new surface-shifted components are attributed to the chemisorbed molecules, since the higher electronegativities of functional groups such as Cl, OH, and COOH in allyl chloride, allyl alchohol, or acryclic acid, as well as the unsaturated $C_2H_2$, will result in a chemically shifted C1s peak at a binding energy. After the adsorption of 1,3-butadiene, however, we were not able to resolve the 1,3-butadiene signal from the bulk C1s. The C1s peak positions of the organic layer

**TABLE 2: Binding Energy (BE) and Intensity of the Chemically Shifted Peak (Attributed to the Adsorption of Molecules) in C1s Core Level Spectra after Saturation Dosage of the Organic Molecules, Measured Relative to the Bulk C1s Signal**

| | surfaces | | organic molecules | | | | |
|---|---|---|---|---|---|---|---|
| | bare diamond C(100) 2 × 1 | H- terminated diamond C(100) 2 × 1:H | 1,3-butadiene | acrylic acid | allyl alcohol | allyl choride | acetylene |
| BE of shifted C1s peak relative to bulk (eV) | | | | 1.14 | 0.73 | 1.22 | 1.09 |
| intensity of the shifted C1s peak relative to bulk (%) | | | | 25.5 | 23.0 | 17.0 | 12.4 |
| BE of bulk C1s (eV) | 285.0 | 284.42 | 284.88 | 284.72 | 284.78 | 284.69 | 284.93 |

relative to the bulk peak, as well as the relative intensity of these new species, are summarized in Table 2. It is noteworthy to point out that the shift in bulk C1s binding energy after dosing with organics suggests a small unbending of the downward bent bands from the clean surface. However the magnitude of this unbending is much smaller than that induced by hydrogen termination. One explanation is that a surface dipole is present in the C−H bonds in the hydrogen-terminated surface, but such a dipole is absent in C−C covalent bonds for the organic adsorbed surface. Parts a−c of Figure 4 show that dosing with oxygen-containing organics such as allyl alcohol and acrylic acid resulted in the growth of the O1s signal with the dosage, and dosing with ally chloride resulted in an increase of the Cl2p signal. These evidence the successful attachment of allyl organics with different functional groups on the bare diamond surface.

**3.2. Allyl Organics Adsorption/Desorption on the Diamond (100) 2 × 1 Surface.** The adsorption and desorption profiles of the allyl organics were studied by recording the HREELS spectrum at intervals after dosing the organics. The HREELS spectra showing the adsorption of allyl alcohol on clean C(100) 2 × 1 are shown in Figure 5a−e, and those for the adsorption of acrylic acid are shown in Figure 6a−f, respectively. The C−H bending and stretching modes increase with dosage on the surface, as expected, and at higher dosage, a small shoulder assignable to C═C appears at 202 meV, assignable to the presence of physisorbed layers. For acrylic acid, the spectra are distinguished by a component at 209 meV assignable to C═O, as well as a visible shift of the C−H stretching toward ∼380 meV at higher coverages. The peak which appears after the adsorption of acrylic acid and allyl alcohol at 366 meV (2930 $cm^{-1}$) can be assigned to the C−H stretching for saturated carbon, while the peak at 380 meV (3040 $cm^{-1}$) can be assigned to the C−H stretching of unsaturated carbon.[13]

After annealing to 100 °C, there is a slight decrease in all intensities of adsorbent-related signals. Meanwhile, the C−H stretching peak is narrowed, and the maximum now shifts back to 366 meV, indicating the desorption of the physisorbed multilayer. The peak intensity decreases significantly after annealing to 200 °C (h in Figures 5 and 6), which suggests similar desorption patterns arising from C−C bond breakages for the allyl organics. Higher than 300 °C, the adsorbates desorbed completely. The desorption profile of all the organics studied in this work follow consistently similar trends; these molecules desorbed by 300 °C from the surface. The desorption process was also confirmed by photoelectron spectroscopy. The decreasing signals of O1s and Cl2p, for allyl alcohol, acrylic acid, and allyl chloride, respectively, parallel the vanishing intensity of the C−H stretch in HREELS after the diamond crystal was annealed to 300 °C.

In Figures 7 and 8, we show the changes in the C1s core level and valence band after clean diamond was dosed with acrylic acid to saturation coverage. In the core level spectra in Figure 7, the uptake of acrylic acid on the surface resulted in the decrease in the intensities of the dimer signal S1 and an increase of the intensities of the surface-shifted component S2. At saturation coverages, the dimer signal S1 vanished completely, to be replaced by the surface-shifted component S2

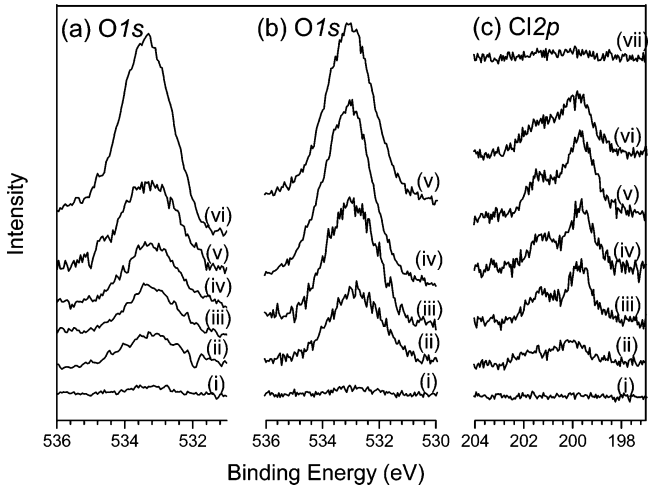


**Figure 4.** (a) Evolution of O1s signal on (i) C(100) 2 × 1, and after dosing with (ii) 10, (iii) 100, (iv) 1000, (v) 5000, and (vi) 10 000 L of allyl alcohol on the surface; (b) evolution of an O1s signal on (i) C(100) 2 × 1, and after dosing with (ii) 10, (iii) 100, (iv) 1000, and (v) 10 000 L of acrylic acid on the surface; (c) evolution of a Cl2p signal on (i) C(100) 2 × 1, after dosing with (ii) 10, (iii) 100, (iv) 1000, and (v) 10 000 L of allyl chloride on the surface, and after subsequent annealing to (vi) 200 and (vii) 300 °C.

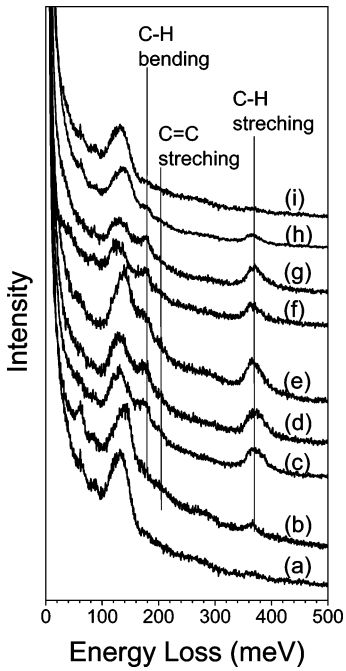


**Figure 5.** HREELS spectra of (a) bare diamond surface; after dosing with (b) 10, (c) 100, (d) 1000, and (e) 10 000 L of allyl alcohol on the diamond surface; and after subsequent annealing to (f) 50, (g) 100, (h) 200, and (i) 300 °C.

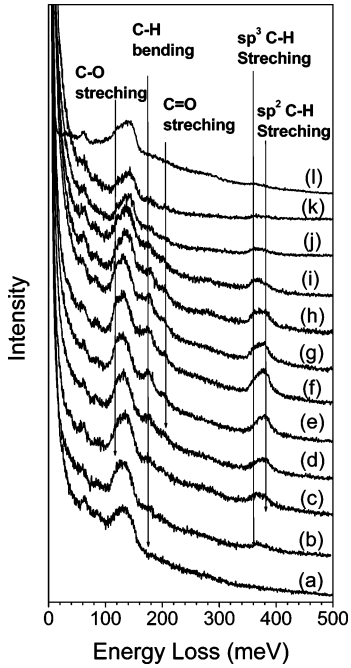


**Figure 6.** HREELS spectra of (a) the bare diamond surface; after dosing with (b) 10, (c) 100, (d) 1000, (e) 5000, and (f) 10 000 L acrylic acid on diamond surface; and after subsequent annealing to (g) 50, (h) 100, (i) 200, (j) 300, (k) 400, and (l) 600 °C.

assignable to carbon atoms of acrylic acid. Similar trends were also observed for the surface dimer in the valence band spectra in Figure 8. The valence spectrum of the clean diamond is characterized by an increase in density of states near the valence band edge (1.7 eV from $E_F$) due to the presence of the $\pi$-bonded surface dimer states. The valence peaks at 5 and 8 eV are characteristics of p states as well as mixed s−p states of bulk diamond, while a peak at 13 eV is a fingerprint of the $sp^3$ bonding in the single crystalline diamond.[33,34] The surface dimer peak becomes attenuated with increasing adsorption of acrylic acid. At the same time, there is a growth of an emission feature at ~11 eV, which is assignable to C2p states of the adsorbed acrylic acid. Figure 9 shows the changes in the core level and valence band spectra after the dosed surface was annealed to successively higher temperatures. After heating to 300 °C, there is a complete decline in the C2p signal and also vanishing of the surface-shifted component in the core level spectrum due to acrylic acid. However, the surface dimer peak S1 in the core level spectrum, as well as its counterpart in the valence band spectrum, did not re-appear until additional heating to 600 °C, suggesting that the diamond surface became disordered after the desorption of the chemically bonded adlayer and required thermal activation for reconstruction. This is further proof that the organics were chemically adsorbed on the reconstructed diamond surfaces and formed covalent bonds with the surface dimer atoms.

**3.3. Acetylene Adsorption/desorption on the Diamond (100) 2 × 1 Surface.** The HREELS spectra in Figure 10 show that the adsorption of acetylene on bare diamond produces new vibration modes such as C═C and $sp^2$ C−H stretching (382.1 meV). Since the adlayer is thermally stable to 200 °C, we believe that acetylene forms a chemisorbed layer. The C1s core level spectra in Figure 11 shows that the adsorption of acetylene results in a chemically shifted C1s peak at 1 eV from the bulk peak, which we assign to the unsaturated C═C bonds in acetylene. It is noteworthy that even after a 100 000 L dose of acetylene on the surface, peaks due to the surface dimers of the clean surface did not disappear, suggesting that the sticking probability of acetylene on the surface is very low.

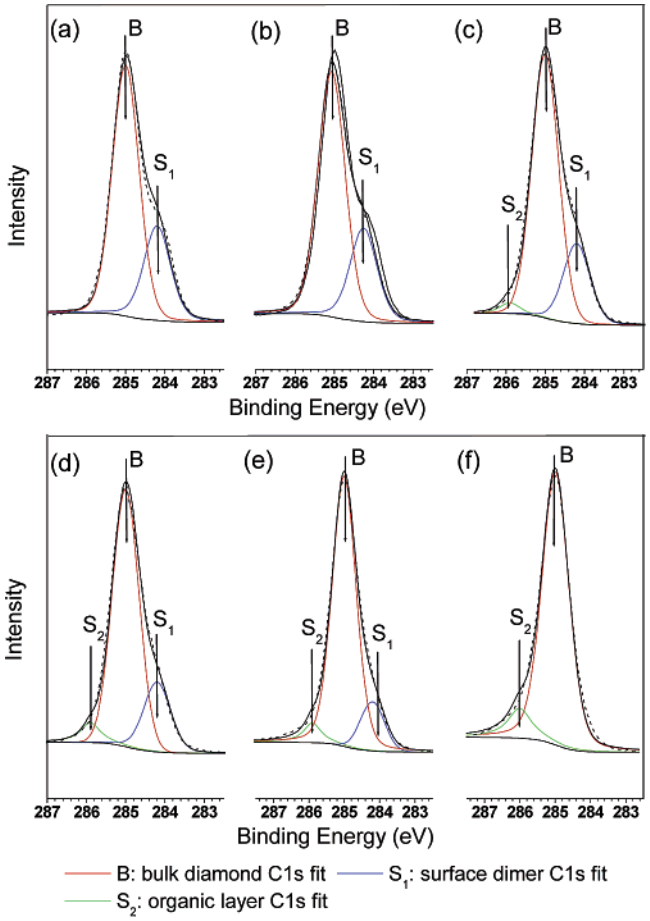


**Figure 7.** C1s core level spectra of (a) bare diamond and after dosing with (b) 5, (c) 10, (d) 100, (e) 1000, and (f) 10 000 L of acrylic acid on the surface. B: C1s of the diamond bulk. $S_1$: C1s of the C(100) 2 × 1 surface dimer. $S_2$: C1s of acrylic acid chemisorbed on the diamond surface.

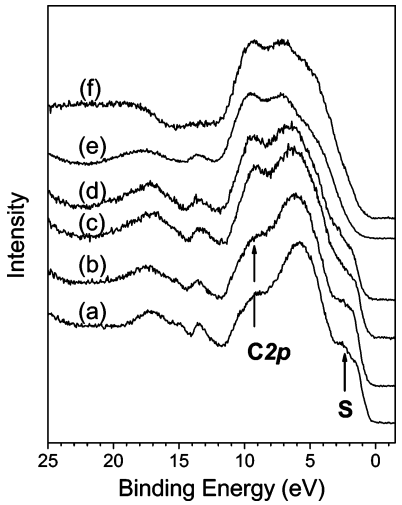


**Figure 8.** Valence band structure collected at off-emission angle (a) C(100) 2 × 1; and after dosing with (b) 5, (c) 10, (d) 100, (e) 1000, and (f) 10 000 L of acrylic acid on the surface. S: surface state of clean C(100) 2 × 1.

**3.4. Adsorption and Desorption of 1,3-Butadiene.** Figure 12 shows the HREELS spectrum for the adsorption of 1,3-butadiene on clean C(100) 2 × 1. The spectrum of adsorbed butadiene shows much stronger C−H bending and stretching

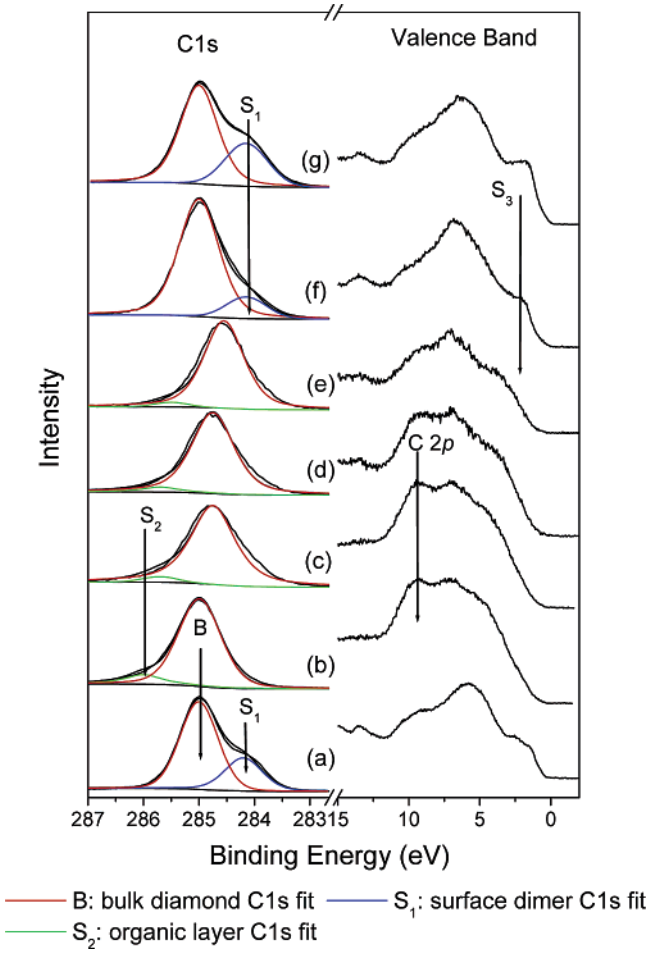


**Figure 9.** C1s core level and valence band spectra of (a) C(100) 2 × 1, and after dosing with 10 000 L of acrylic acid molecules; and subsequent annealing to (c) 100, (d) 200, (e) 300, (f) 600, and (c) 900 °C. B: C1s of bulk diamond. $S_1$: surface dimer signal in C1s. $S_2$: adsorbed acrylic acid in C1s. $S_3$: surface state in the valence band.

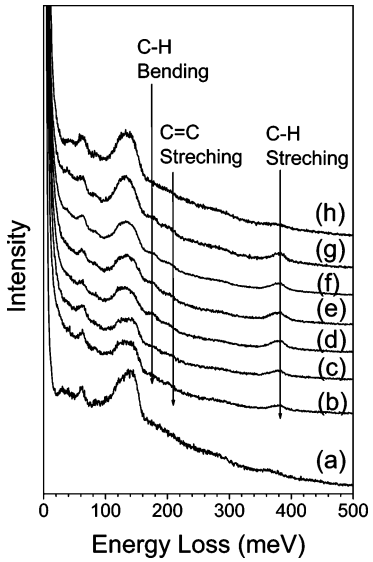


**Figure 10.** HREELS spectra of (a) C(100) 2 × 1; after dosing with (b) 100, (c) 1000, (d) 10 000, and (e) 50 000 L of acetylene; and after subsequent annealing to (f) 100, (g) 200, and (h) 300 °C.

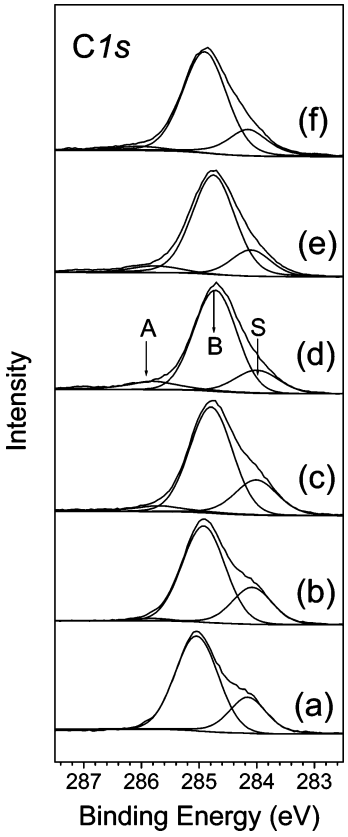


**Figure 11.** C1s core level spectra of (a) C(100) 2 × 1; after dosing with (b) 1000, (c) 10 000, and (d) 100 000 L of acetylene on the surface; and after subsequent annealing to (b) 150 and (c) 300 °C. B: bulk diamond signal. S: dimer signal. A: acetylene signal.

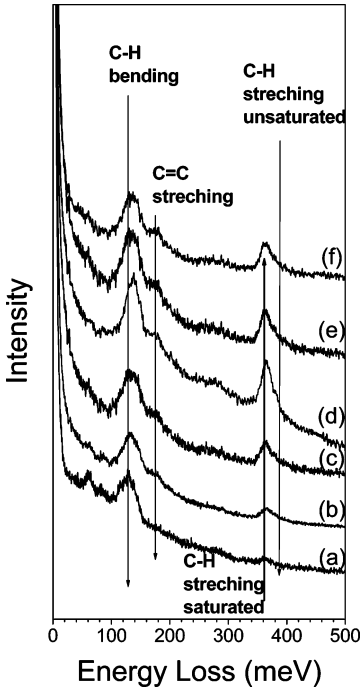


**Figure 12.** HREELS spectra of (a) C(100) 2 × 1; after dosing with (b) 10, (d) 100, and (d) 1000 L of 1,3-butadiene; and after subsequent annealing to (e) 200 and (f) 400 °C.

peaks compared to the other organics used in this work, with dosage levels which are 1−10% of the saturation dosages usually employed for the other organic molecules. Due to the sharper C−H bending modes at 140 meV, its overtone can be observed as a broad signal at 280 meV. This feature is also observed for the hydrogenated diamond, but otherwise absent in the HREELS spectra of other organic systems due to the much weaker C−H bending signals. The desorption temperature

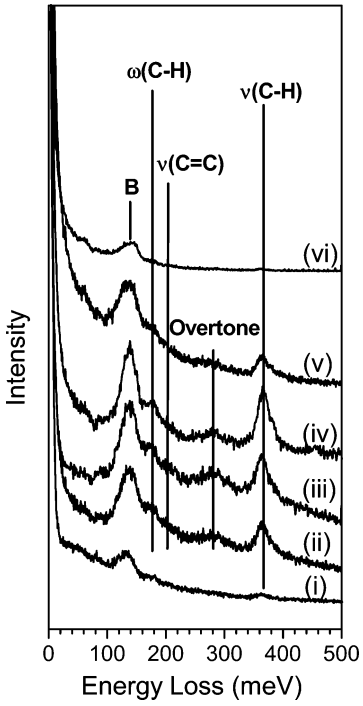


**Figure 13.** Plot of loss intensities for different primary beam energies ($E_p$) after saturation dosage of 1,3-butadiene on diamond C(100), with $E_p$ of (i) 3, (ii) 5, (iii) 7, (iv) 8, (v) 10, and (vi) 15 eV. B: bulk phonon TO at X.

of 1,3-butadiene was observed to be higher than 400 °C, whereas all the other organics desorbed by 300 °C. This suggests that 1,3-butadiene has a higher sticking probability compared to the other organic molecules and that the adlayer formed on the diamond surface is more stable than all other organic adsorbates considered in this work. Figure 13 shows the plot of loss intensities versus primary beam energy; interestingly, the same resonance scattering profile observed for hydrogenated C(100) 2 × 1−H can be observed for 1,3-butadiene. Previously we associated this resonance scattering with a NEA surface where electrons can be scattered more efficiently from the conduction band; we will show in a later section that the 1,3-butadiene-dosed surface indeed exhibits the condition of NEA.

Figure 14 shows the changes in the valence band spectrum of the clean diamond collected at normal and off-normal emission following exposures to 1,3-butadiene. There are observable differences in peak intensities in these two cases, which can be explained by the more directional nature of the p orbitals from the dimer states of reconstructed diamond (1.7 eV) as well as carbon 2p signals of bulk diamond (11 eV), as these emission states appear stronger at normal emission compared to off-normal emission. At off-normal emission, the C2p of the adsorbed adlayer can be seen clearly as these are not masked by the bulk diamond signal, and the peak intensity grows with increasing coverage of 1,3-butadiene on the surface; this is accompanied by the attenuation of the surface dimer peak at 1.7 eV. Figure 15 shows the changes in the corresponding C1s core level spectra. Similar to previous adsorption cases, exposure to 1,3-butadiene attenuates the emission due to the dimer state; however, no other chemically shifted component can be seen even at saturation exposures due possibly to the overlap of similar spectral features between the adsorbate and bulk.

**3.5. Hydrocarbon-Induced Lowering of Electron Affinity on Diamond (100) 2 × 1.** In this work, we discover that the adsorption of almost all organic molecules (i.e. allyl alcohol,

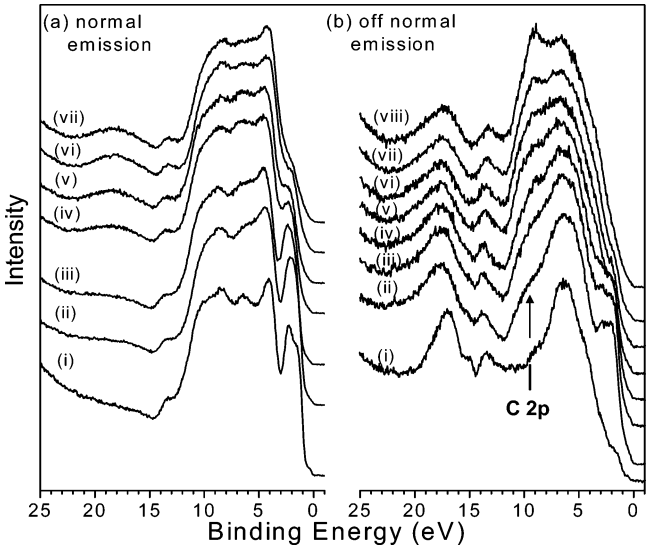


**Figure 14.** Valence band of C(100) 2 × 1 after exposure to 1,3-butadiene with (a) normal emission, from bottom up: (i) bare diamond, and after dosing with (ii) 1, (iii) 10, (iv) 100, (v) 500, (vi) 1000, and (vii) 2000 L; with (b) off-normal emission, from bottom up: (i) hydrogenated diamond, (ii) bare diamond, and after dosing with (iii) 1, (iv) 10, (v) 100, (vi) 500, (vii) 1000, and (viii) 2000 L.

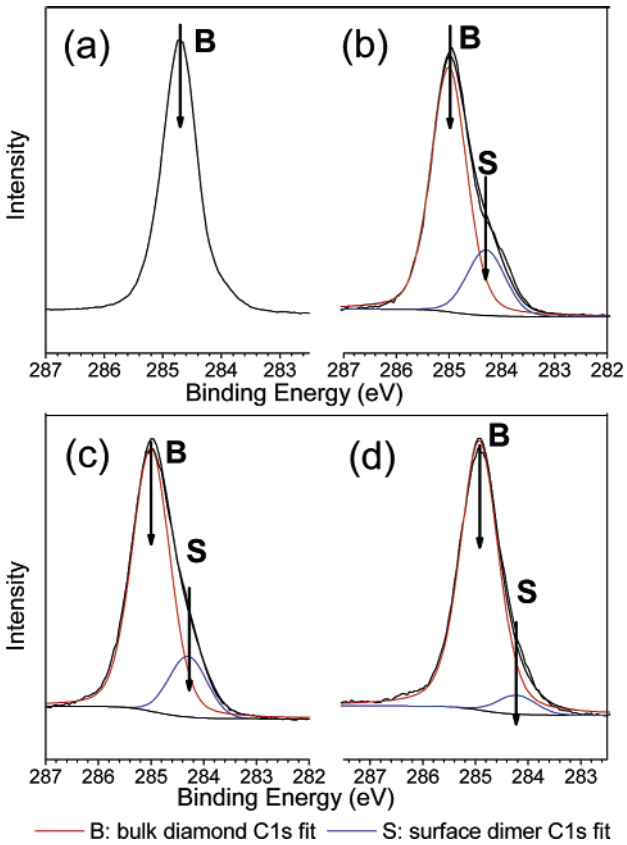


**Figure 15.** C1s spectra of (a) C(100) 2 × 1−H, (b) C(100) 2 × 1; and after dosing with (c) 100 and (d) 1000 L of 1,3-butadiene.

acrylic acid, acetylene, and 1,3-butadiene, etc) on the diamond C(100) 2 × 1 surface lowered the electron affinity of the surface from the positive electron affinity (PEA) condition and enhanced secondary electron emission significantly. This phenomena was studied by analyzing the low-energy cutoff in the photoelectron spectra using the synchrotron light source at $h\nu = 60$ eV. The low-energy cutoff in the secondary electron emission originates from the conduction band minimum (CBM) in the event of

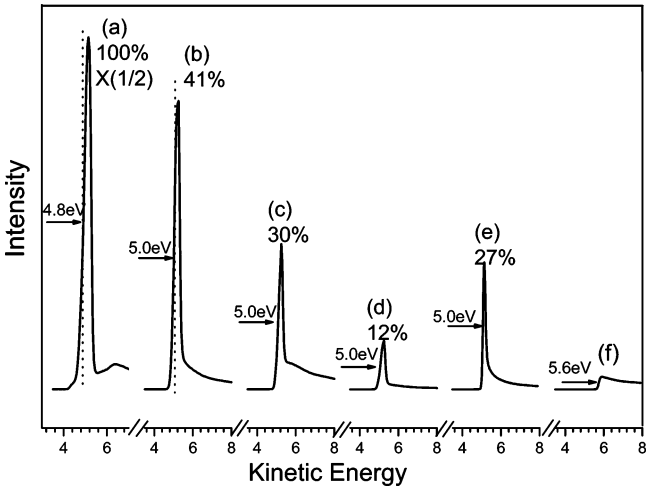


**Figure 16.** Secondary electron emission spectra of (a) C(100) 2 × 1−H, and after saturated dosing of (b) 1,3-butadiene, (c) allyl alcohol, (d) acrylic acid, and (e) acetylene; (f) Spectrum of bare diamond C(100) 2 × 1.

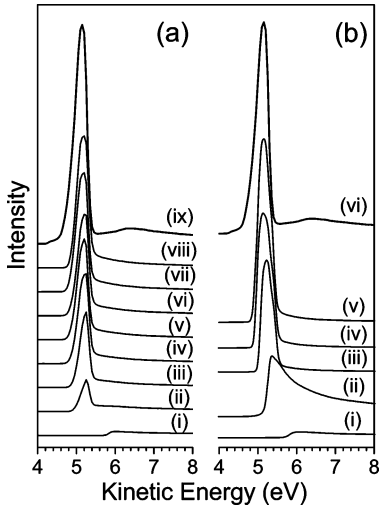


**Figure 17.** Secondary electron emission spectra. (a) (i) C(100) 2 × 1, and after dosing with (ii) 10, (iii) 100, and (iv) 1000 L of 1,3-butadiene, followed by annealing to (v) 60, (vi) 100, (vii) 200, and (viii) 300 °C. (ix) C(100) 2 × 1−H for comparison. (b) (i) C(100) 2 × 1, and after dosing with (ii) 10 000 L of allyl alcohol, followed by annealing to (iii) 60, (vi) 100, (v) 200, and (vi) 300 °C. (vii) Spectrum of C(100) 2 × 1−H for comparison.

NEA.[22−26] Secondary electrons which are excited into the conduction band states rapidly thermalize down to the CBM and spontaneously escape if the vacuum level is positioned beneath the CBM. For PEA, secondary electrons escape from states above the vacuum level. Therefore for a p-type semiconductor with NEA, the peak of the low-energy cutoff, when referenced to the Fermi level, is expected to be less than or equal to the band gap energy (5.5 eV). The secondary electron yield from the NEA surface will also be significantly higher due to the higher probability of escape.

The secondary electron emission spectra (vacuum cutoff of the spectra) are shown in Figure 16 for H-terminated and bare diamond and after saturation dosages of the various organic molecules. The bare surface has a very weak secondary electron peak with an intensity that is less than 5% of the hydrogen-terminated surface. The low-energy cutoff is situated at ∼6 eV, compared to ∼5.2 eV for the hydrogenated surface. Thus it is obvious that the bare surface has the condition of PEA, while the hydrogenated diamond surface may have NEA. Interestingly, dosing the various organic molecules at room temperature also lowers the electron affinity of the diamond surface, by as much as 0.8 eV. As shown in Figure 16, the intensity of the secondary electron peak was increased from that of the clean surface; according to the descending order of their relative intensities, we have 1,3-butadiene, allyl alcohol, acetylene, and acrylic acid. 1,3-Butadiene was found to show the strongest enhancement of the secondary electron emission condition for room temperature adsorption after saturation exposures. Figure 17a shows the change in the secondary electron yield when 1,3-butadiene was dosed onto the diamond surface, followed by thermal annealing to investigate the effect on the secondary electron yield. After saturation dosage of butadiene, the secondary yield obtained was only 40% of the H-terminated surface. However, after annealing to 150 °C, the secondary electron yield reached 70% of the H-terminated diamond surface. This may be attributed to the dissociation of the C−H bonds of the adsorbed layers at higher temperature, resulting in partial hydrogen coverage of the diamond surface. The same trends were observed for the other organic system like allyl alcohol (Figure 17b) in that the secondary electron yield increases upon annealing the adlayer to elevated temperatures above 150 °C. We are not able to detect from HREELS or electron spectroscopy the changes in the chemical bonding of the adlayer following annealing, but we suppose that the dehydrogenation of the surface adsorbate may change the adlayer characteristics, i.e., polymerization or increasing unsaturation.

**3.6. X-ray Adsorption Spectroscopy Study.** The dimer rows on C(100) 2 × 1 can potentially act as a template for ordered assembly of organic layers. The orientation of dimer has been confirmed in our study by angle-dependent near-edge X-ray adsorption measurements (NEXAFS) in Figure 18a. The 283.5 eV exciton observed on bare diamond is related to the antibonding $\pi^*_{C-C}$ orbital[35] of the surface dimer, and the higher peak intensity at more grazing incidence of the polarized X-ray suggests that the p-orbital is oriented parallel to the surface normal. A small preedge peak located at 286 eV is assigned to the C−H $\sigma^*$ state; in a, it is due to residual surface hydrogen, and this peak is stronger in the hydrogenated diamond surface, as can be seen in b. The resonant scattering observed in HREELS for hydrogenated diamond may be due to scattering into unfilled C−H $\sigma^*$ states which are above the vacuum level in the case of NEA. Parts c and d of Figure 18 show that the adsorption of acetylene and 1,3-butadiene, respectively, on the surface attenuates the 283.5 eV exciton significantly, indicating the destruction of surface $\pi$ bonds in $\sigma$ bond formation. In c, only a weak $\pi^*_{C-C}$ peak at 284 eV can be observed for acetylene-dosed diamond, which increases in intensity with incident X-ray angle. However, the $\pi^*_{C-C}$ peak in the case of diamond dosed with 1,3-butadiene shows no angular dependence.

## 4. Discussion

The chemisorption of allyl organics, 1,3-butadiene, and acetylene on diamond C(100) 2 × 1 has been verified in this study by HREELS and photoelectron spectroscopy. All the adsorbates remained stable to 300 °C, while 1,3-butadiene is thermally stable to temperatures above 400 °C, which suggests that covalent bonds were involved in the adsorption as opposed to weakly bound physisorbed layers. The attenuation of the dimmer state-related peaks observed in the C1s core level peaks as well as valence band spectra following the exposures to these organic molecules is due to the breaking of the dimer $\pi$ bonds on the diamond surface and formation of $\sigma$ bonds between the

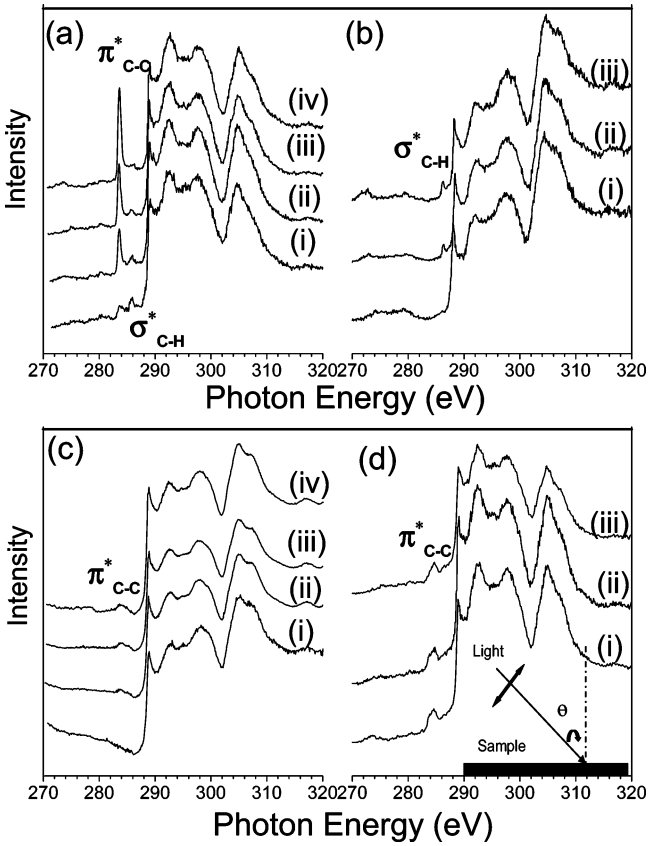


**Figure 18.** Near-edge X-ray absorption spectra of (a) C(100) 2 × 1 with incident X-ray angles of (i) 0, (ii) 35, (iii) 52, and (iv) 67°; (b) same as a but for C(100) 2 × 1−H; (c) after saturation dose with acetylene; and (d) after saturation dose with 1,3-butadiene, with incident X-ray angles of (i) 0, (ii) 50, and (iii) 60°.

diamond and the adsorbing organics. This suggests that adsorption was not restricted to defect sites on the surface. If we use either the ratio of the C−H stretching peak to the elastic peak or the secondary electron yield from the surface following the adsorption of the organic molecules as a rough gauge of surface coverage, 1,3-butadiene shows the highest coverage on the diamond surface (1000 L dose) among all the organic molecules considered in this work and acetylene shows the lowest coverage (100 000 L dose), at their respective saturation dosages. One possible reaction between allyl organics (or acetylene) and diamond C(100) 2 × 1 is the [2+2] type cycloadditions; for 1,3-butadiene, it can follow either the [2 + 2] or [4 + 2] type cycloaddition. Another possibility is the end conjugation of the organic molecule to the surface dimer bonds; in this case the surface dimer atoms can act as diradical with one radical initiating the attack on the unsaturated bonds in the organic molecules. By either mechanism, the $\pi$ bonding in the surface dimer will be broken, to be replaced by $\sigma$ bonds, which explains the attenuation of the dimmer state-related features in the C1s core level or valence band spectrum following exposures to these organics. The suggested reaction scheme for [2 + 2] type cycloadditions is shown in Figure 19. For organic molecules such as 1,3-butadiene and acetylene, unsaturation can occur in the molecules after bonding and bond rearrangement. The higher coverage of 1,3-butadiene and greater thermal stability on C(100) 2 × 1 compared to the rest of the organic systems suggest that it most possibly bonds differently compared to the rest, since it is the only species here that can undergo [4 + 2] type cycloaddition. Without considering the symmetry of the reacting frontier orbitals, but focusing our attention on the

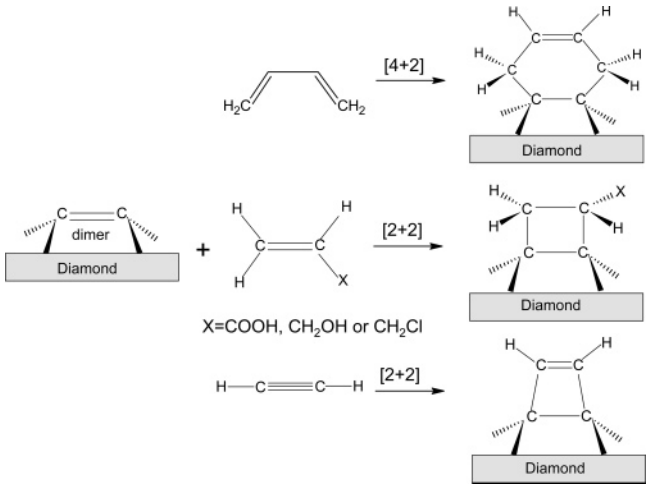


**Figure 19.** [2 + 2] cycloadditions for 1,3-butadiene, allyl ornics and acetylene on the C(100) 2 × 1 surface.

stability of the adduct formed on a solid template with a restricted degree of in-plane freedom, it can be appreciated quite readily that the [4 + 2] adduct of 1,3-butadiene can bond to the diamond dimer atoms with more relaxed C−C bond angles, compared to the strained four-membered ring of the [2 + 2] adduct. The bonding of 1,3-butadiene on C(100) 2 × 1 had been observed by Hossain and co-workers and assigned to [4 + 2] type cycloaddition,[11] but they failed to observe the [2 + 2] cycloadditions of acetylene or ethylene on diamond.

Fan et al.[36] suggested that there are exceptions to the Woodward−Hoffmann rules for surface [2 + 2] cycloadditions, especially when applied to an extended solid-phase system. In contrast to molecular systems where electron transfer occurs from discrete orbitals, electron transfer can proceed from a continuum of states in solid systems. When orbital interactions between two reactants leads to crossing over the Fermi level, electron transfer can proceed; as a result the surface reaction is very different from the gas-phase counterpart. We have tested the reactions of allyl alcohol on heavily boron-doped polycrystalline diamond and found that the reaction probabilities in this case are higher than that on single crystalline diamond, suggesting that the Fermi level of the reacting solid has a definite influence on the [2 + 2] reaction probabilities. Alternatively, due to the presence of a functional group like OH, or COOH, in the allyl organics, an asymmetric [2 + 2] pathway is likely. In this mechanism, the formation of a $\pi$ complex, or a diradical intermediate with one end of the reactant first conjugated to the surface $\pi$ bonds, has also been suggested.

Our NEXAFS study shows that the $\pi^*$ orbitals of adsorbed acetylene show similar angular dependence as the diamond surface $\pi$ bonds, indicating that it is adsorbed with its bond axis in the plane of the diamond surface; it is most probably a [2 + 2] adduct. Although it is beyond the scope of this work to provide accurate quantitative sticking probability measurement, we can judge from both the weaker C−H loss intensity in HREELS and the weaker $\pi^*$ exciton peak in NEXAFS that the surface coverage of acetylene is significantly lower than that of 1,3-butadiene. This implies that the reaction probability of the [2 + 2] cycloaddition is much lower than the [4 + 2]. The NEXAFS study detected no angular dependence for the $\pi^*$ orbitals of 1,3-butadiene, indicating that the bonding is disordered. This might be due to the greater flexibility of the six-membered ring in the 1,3-butadiene adduct which introduces varying degrees of in-plane tilt, compared to the more structurally rigid four-membered adduct in acetylene.

This work provides the first documentation that the adsorption of hydrocarbon can lower the electron affinity of the clean diamond significantly. Prior to this, all previous literature in this area focused on the hydrogen-terminated diamond surface. In the case of the hydrogen-terminated diamond surface, the surface dipole of $C^{\delta-}-H^{\delta+}$ can help to lower the surface vacuum level with respect to the CBM. However no such dipole can occur between C−C covalent bonds formed between the adsorbed organic and diamond; core level photoelectron spectroscopy shows that there is no significant change in the condition of band bending on clean diamond following the adsorption of organic molecules, as such changes are expected when there is charge transfer. On the other hand, if we consider the covalently bound organics as an extension of the diamond lattice, then the terminal C−H bonds of organics such as 1,3-butadiene, acetylene, and allyl alcohol have the positive end of the dipole facing the vacuum. The planar average of the electrostatic potential field on the diamond surface will be lowered as a result. The surface bound organics itself can also exhibit true negative electron affinity because the wide separation between the bonding and antibonding orbitals in these molecular systems causes the vacuum level to be beneath the antibonding orbitals. Our measurements show that the secondary electron yield obtained from the hydrocarbon-dosed surface, while significantly higher than that of the bare diamond surface, is, however, lower than that of hydrogenated diamond for all molecules studied here. One explanation is that the steric hindrance from these larger molecules precludes a high-density surface coverage similar to hydrogen termination. The highest secondary yield observed for room temperature adsorption was about 40% that of the hydrogenated surfaces, and that was obtained from the surface dosed with 1,3-butadiene. We previously explained that this molecule has a higher sticking probability on diamond, possibly due to the symmetry-favored [4 + 2] cycloaddition.

## 5. Conclusion

Using HREELS and photoemission spectroscopy, we have shown that allyl alcohol, acrylic acid, and allyl chloride, as well as acetylene and 1,3-butadiene, chemisorb on the clean diamond C(100) 2 × 1 surface. The fact that [2 + 2] cycloaddition products can be formed on this surface suggests that surface reactions are exceptions to the Woodward−Hoffmann rules. However, 1,3-butadiene which can undergo [4 + 2] cycloaddition has a higher reaction probability with the diamond surface and gives a more thermally stable adsorbate. The adsorption of all organic molecules on the clean surface is found to lower the electron affinity of the surface significantly. The secondary electron yield obtained is significantly higher than that of the bare surface but is less than that of the hydrogenated diamond surface due to the lower surface coverage.

## References and Notes

(1) Hamers, R. J.; Butler, J. E.; Lasseter, T.; Nichols, B. M.; Russell, J. N.; Tse, K. Y.; Yang, W. S. *Diamond Relat. Mater.* **2005**, *14*, 661.

(2) (a) Kawarada, H.; Araki, Y.; Sakai, T.; Ogawa, T.; Umezawa, H. *Phys. Status Solidi A* **2001**, *185*, 79. (b) Minoru, T.; Kaibara, Y.; Sumikawa, Y.; Kawarada, H. *Phys. Status Solidi A* **2003**, *199*, 39.

(3) Hartl, A.; Schmich, E.; Garrido, J. A.; Hernando, J.; Catharino, S. C. R.; Walter, S.; Feulner, P.; Kromka, A.; Steinmuller, D.; Stutzmann, M. *Nat. Mater.* 2004, *3*, 736.

(4) Garrido, J. A.; Hardl, A.; Kuch, S.; Stutzmann, M.; Williams, O. A.; Jackmann, R. B. *Appl. Phys. Lett.* **2005**, *86*, 073504.

(5) Cui, J. B.; Stammer, M.; Ristein, J.; Ley, L. *J. Appl. Phys.* **2000**, *88*, 3667

(6) Ristein, J.; Maier, F.; Riedel, M.; Stammer, M.; Ley, L. *Diamond Relat. Mater.* **2001**, *10*, 416.

(7) Riedel, M.; Ristein, J.; Ley, L. *Phys. Rev. B* **2004**, *69*, 125338.

(8) Jian, W.; Firestone, M. A.; Auciello, O.; Carlisle, J. A. *Langmuir* **2004**, *20*, 11450.

(9) Strother, T.; Knickerbocker, T.; Russel, J. N.; Butler, J. E.; Smith, L. M.; Hamers, R. J. *Langmuir* **2002**, *18*, 968.

(10) Knickerbocker, T.; Strother, T.; Schwartz, M. P.; Russell, J. N.; Butler, J.; Smith, L. M.; Hamers, R. J. *Langmuir* **2003**, *19*, 1938.

(11) Hossain, M. Z.; Aruga, T.; Takagi, N.; Tsuno, T,; Fujimori, N.; Ando, T.; Nishijima, M. *Jpn. J. Appl. Phys.* **1999**, *38*, 1496.

(12) Wang, G. T.; Bent, S. F.; Russell, J. N.; Butler, J. E.; D'Everlyn, M. P. *J. Am. Chem. Soc.* **2000**, *122*, 744.

(13) Hovis, J. S.; Coulter, S. K.; Hamers, R. J.; D'Everlyn, M. P.; Russell, J. N.; Butler, J. E. *J. Am. Chem. Soc.* **2000**, *122*, 732.

(14) Sorescu, D. C.; Jordan, K. D. *J. Phys. Chem. B* **2000**, *104*, 8259.

(15) Lu, X. *J. Am. Chem. Soc.* **2003**, *125*, 6384.

(16) Lu, X.; Zhu, M. *Chem. Phys. Lett.* **2004**, *393*, 124.

(17) Cho, J. H.; Kleinman, L. *Phys. Rev. B* **2003**, *68*, 195413.

(18) Cho, J. H.; Kleinman, L. *Phys. Rev. B* **2004**, *69*, 075303.

(19) Carbone, M. *J. Am. Chem. Soc.* **2000**, *122*, comment on ref 13.

(20) Maier, F.; Riedel, M.; Mendel, B.; Ristein, J.; Ley. L. *Phys. Rev. Lett.* **2000**, *85*, 3472.

(21) Ristein, J.; Riedel, M.; Maier, F.; Stammler, M.; Ley, L. *J. Phys. Condens. Matter* **2001**, *13*, 8979.

(22) Bandis, C.; Pate, B. B. *Phys. Rev. B* **1995**, *52*, 12056.

(23) Bandis, C.; Pate, B. B. *Surf. Sci.* **1996**, *350*, 315.

(24) Diederich, L.; Küttel, O. M.; Schaller, E.; Schlapbach, L. *Surf. Sci.* **1996**, *349*, 176.

(25) Diederich, L.; Küttel, O. M.; Ruffieux, P.; Pillo, Th.; Aebi, P.; Schlapbach, L. *Surf. Sci.* **1998**, *417*, 41.

(26) Maier, F.; Ristein, J.; Ley, L. *Phys. Rev. B* **2001**, *64*, 165411.

(27) Takeuchi, D.; Ri, S.-G.; Kato, H.; Nebel, C. E.; Yamasaki, S. *Phys. Status Solidi A* **2005**, *202*, 2098.

(28) Yu, X. J.; Wilhelmi, O.; Moser, H. O.; Vidyaraj S. V.; Gao X. Y.; Wee, A. T. S.; Nyunt, T.; Qian, H. J.; Zheng, H. W. *J. Electron. Spectrosc. Relat. Phenom.* **2005**, *144*, 1031.

(29) Thachepan, S.; Okuyama, H.; Agura, T.; Nishijima, M.; Ando, T.; Mazur, A.; Pollmann, J. *Phys. Rev. B* **2003**, *68*, 041401.

(30) Alfonso, D. R.; Drabold, D. A.; Ulloa, S. E. *Phys. Rev. B* **1995**, *51*, 1989.

(31) Hossain, M. Z.; Kubo, T.; Aruga, T.; Takagi, N.; Tsuno, T,; Fujimori, N.; Nishijima, M. *Jpn. J. Appl. Phys.* **1999**, *38*, 6659.

(32) Fally, F.; Virlet, I.; Riga, J.; Verbist, J. *J. Appl. Polym. Sci.* **1996**, *59*, 1569.

(33) Zheng, J. C.; Xie, X. N.; Wee, A. T. S.; Loh, K. P. *Diamond Relat. Mater.* **2001**, *10*, 500.

(34) Loh, K. P.; Xie, X. N.; Lim, Y. H.; Teo, E. J.; Zheng, J.; Ando, T. *Surf. Sci.* **2002**, *505*, 93.

(35) Bobrov, K.; Comete, G.; Dujardin, G.; Hellner, L.; Bergonzo, P.; Mer, C. *Phys. Rev. B* **2001**, *63*, 165421.

(36) Fan, X. L.; Zhang, Y. F.; Lau, W. M.; Liu, Z. F. *Phys. Rev. B* **2005**, *72*, 165303.